

# Morphologic and Doppler Findings from Hepatic Ultrasonography of Normal Cynomolgus Monkeys (*Macaca fascicularis*)

Kyo Won Lee,<sup>1</sup> Chan Woo Cho,<sup>1</sup> Ji Eun Lee,<sup>2</sup> Hyojun Park,<sup>1</sup> Gyu-Seong Choi,<sup>1</sup> Woo Kyoung Jeong,<sup>2</sup> Jae Berm Park,<sup>1</sup> and Sungjoo Kim<sup>1,\*</sup>

The present study evaluated the anatomic and ultrasonographic features of the liver in normal cynomolgus monkeys (*Macaca fascicularis*). Healthy, male, cynomolgus monkeys from Cambodia ( $n = 25$ ; mean age, 58.1 mo) were sedated with ketamine (7 mg/kg) and examined by using 2D and Doppler ultrasonography. We measured the diameters of the vascular structures and bile duct, determined the velocities of the hepatic artery and portal vein, and calculated the resistance index of the hepatic artery. Vessel diameters were: proper hepatic artery, 1.4 mm (range, 1.0–1.9 mm); main portal vein, 4.4 mm (range, 2.4–6.0 mm); and common bile duct, 1.5 mm (range, 1.0–2.4 mm). The mean peak systolic velocity of the proper hepatic artery was 75.4 cm/s, and the resistance index was 0.54. The mean velocity of the main portal vein was 19.3 cm/s. All Doppler ultrasonographic findings, including the peak systolic velocity, end-diastolic velocity, and resistance index of the proper hepatic artery and the main portal vein velocity were independent of body weight. These findings have the potential to serve as references for determining the health status of the liver from cynomolgus monkeys.

**Abbreviations:** MPV, main portal vein; PHA, proper hepatic artery

The acquisition of immunologic tolerance has been the major issue in the field of organ transplantation for decades. Experiments in rodents and NHP have improved our understanding of this phenomenon.<sup>6,9,10,13</sup> However, additional studies are necessary to achieve immunologic tolerance in the clinical setting. The liver is the most tolerogenic solid organ and exhibit lower rejection rates and immunosuppressant requirements than do other solid-organ transplants, such as kidney, heart, and lung.<sup>7</sup> The high tolerogenicity of the liver is due to the presence of resident immunocytes and antigen-presenting cells, which are regulatory in nature and protect against graft injury and rejection; of various proteins (for example, HLA-G) and cytokines produced from extramedullary hematopoietic stem cells; and of the large number of nonhematopoietic, support cells (for example, hepatocytes, stellate cells, and endothelial cells). By exploiting this phenomenon of tolerogenicity, recent studies have used animal models of liver transplantation to investigate new strategies for immune system modulation.<sup>9–11</sup> Doppler ultrasonography plays a key role in the postoperative monitoring of liver transplant recipients, allowing for patency evaluation of the portal vein, hepatic artery, and hepatic vein. Cynomolgus monkeys (*Macaca fascicularis*) are frequently used for transplant research because of their anatomic, physiologic, and pathophysiologic similarity to humans. However, no reports detailing the ultrasonographic findings of the liver in normal cynomolgus monkeys that can be used as references have been published.

The objective of this study was to use 2D and Doppler ultrasonography to obtain normal sonographic parameters of the

liver in young adult male cynomolgus monkeys. The measured sonographic values can serve as references for further transplant studies that examine the liver in cynomolgus macaques.

## Materials and Methods

All procedures were conducted in accordance with the *Guide for the Care and Use of Laboratory Animals*<sup>5</sup> and the Animal Welfare Act<sup>1</sup> in the animal facility of the Nonhuman Organ Transplantation Research Center at Genia (Seong-nam City, Korea). The animal protocol was approved by the IACUC of Genia (ORIENT-IACUC-16052).

**Animals.** From March through June 2016, the livers of healthy, ketamine-sedated, male cynomolgus monkeys (*Macaca fascicularis*;  $n = 25$ ; mean age, 58.1 mo [range, 45 to 79 mo]; mean weight, 4.6 kg [range, 3.2 to 6.8 kg]) from Cambodia were examined using 2D and power Doppler. Animals were individually housed indoors on a 12:12-h light:dark cycle and were fed standard macaque biscuits (Harlan Laboratories, Seoul, Korea) and fresh fruit twice daily. Hematology and serum chemistry results were within normal limits for all animals. In addition, the monkeys were negative for tuberculosis, viral serology (herpes B virus, simian T-lymphotropic virus, SIV, simian type D retrovirus, and hepatitis B virus), *Salmonella* (*Shigella*), and fecal parasites.

**Preparation for ultrasonography examination.** After a 12-h fast, sedation was induced with ketamine (7 mg/kg IM; Daiichi Sankyo, Ltd, Tokyo, Japan). Blood pressure, body temperature, and oxygen saturation ( $\text{SpO}_2$ ) were monitored throughout sedation of each monkey. The blood pressure was measured by using an arm cuff. The mean systolic blood pressure was 108.6 mm Hg (range, 88 to 131), and the mean diastolic blood pressure was 57.7 mm Hg (range, 30 to 89); both of these parameters were within normal limits.  $\text{SpO}_2$  values were also within their respective normal ranges. Body temperature, which remained within normal limits (37 to 39 °C), was monitored with a rectal

Received: 28 Sep 2016. Revision requested: 28 Oct 2016. Accepted: 18 Nov 2016.  
Departments of <sup>1</sup>Surgery and <sup>2</sup>Radiology and Center for Imaging Science, Samsung Medical Center, Sungkyunkwan University School of Medicine, Seoul, Korea  
\*Corresponding author. Email: kmhyj111@gmail.com

probe and maintained by using a heat-circulating blanket. SpO<sub>2</sub> was monitored with pulse oximetry at the monkey's ear and remained between 90% and 100%. During the examination, monkeys were restrained on a surgical bed in the supine position. Scans were performed by using a 9L linear transducer and the LOGIQ E9 system (GE Healthcare, Waukesha, WI). All examinations were performed by the same operator.

**2D ultrasonography.** The diameters of the proper hepatic artery (PHA), main portal vein (MPV), right posterior portal vein, right anterior portal vein, left portal vein, right hepatic vein, middle hepatic vein, left hepatic vein, suprahepatic inferior vena cava, infrahepatic inferior vena cava, and bile duct were measured by using the electrical caliper incorporated in the ultrasonic device. During measurements, the transducer was placed transversely to the hepatic pedicle just below the last rib (Figure 1). The parenchymal echogenicity of the liver was compared with that of the right kidney with the transducer parallel to the hepatic pedicle (Figure 1).

**Doppler ultrasonography.** Flow rates within the PHA, MPV, right anterior portal vein, right posterior portal vein, left portal vein, right hepatic vein, middle hepatic vein, and left hepatic vein were identified with the transducer parallel to the hepatic pedicle (Figure 1). The Doppler waveforms were obtained by insonating the PHA, MPV, and hepatic veins at a 60° angle to the ultrasound beam; the sample volume was then placed in the middle of the vessel. Peak systolic and end-diastolic velocities of the PHA were recorded. By using the onboard electronic caliper, the resistance index (RI) of the PHA was calculated as:

$$RI = (PSV - EDV) / PSV,$$

where PSV is the peak systolic velocity and EDV the end-diastolic velocity of the PHA. In addition, the velocity of the blood flow within the MPV was recorded; when slight phasicity due to respiration occurred, the mean velocity was recorded.

**Statistical analysis.** All values are presented as means with ranges for continuous variables. Comparisons between continuous variables were made using Student *t* test. Statistical analysis was performed using SPSS version 22.0 (IBM, Armonk, NY). *P* values were considered significant at 0.05.

## Results

**2D ultrasonographic findings.** The normal liver parenchyma was more hypoechoic than the kidney parenchyma and showed homogenous echogenicity (Figure 2). The diameters of the vessels and common bile duct are summarized in Table 1. Because the PHA, MPV, suprahepatic inferior vena cava, infrahepatic inferior vena cava, and common bile duct are necessarily anastomosed during cynomolgus monkey liver transplantation, we measured each vessel according to the previously reported surgical anatomy of the cynomolgus monkey (Figure 3).<sup>12</sup> The right posterior portal vein and right anterior portal vein branched from the MPV in both bifurcation (*n* = 12, 48%) and trifurcation (*n* = 13, 52%) patterns.

**Doppler ultrasonographic findings.** Doppler ultrasonography allowed for hemodynamic measurement of the hepatic artery, portal vein, and hepatic vein (Figure 4). The hepatic artery showed a pulsatile waveform, whereas the hepatic vein showed a triphasic waveform (large antegrade systolic and diastolic waveform with a retrograde wave due to backward transmission from right atrial pressure changes during the cardiac cycle). The portal vein showed a monophasic waveform in most cases. However, in some cases, the portal vein waveform exhibited phasicity due to respiration or pulsation of the adjacent hepatic

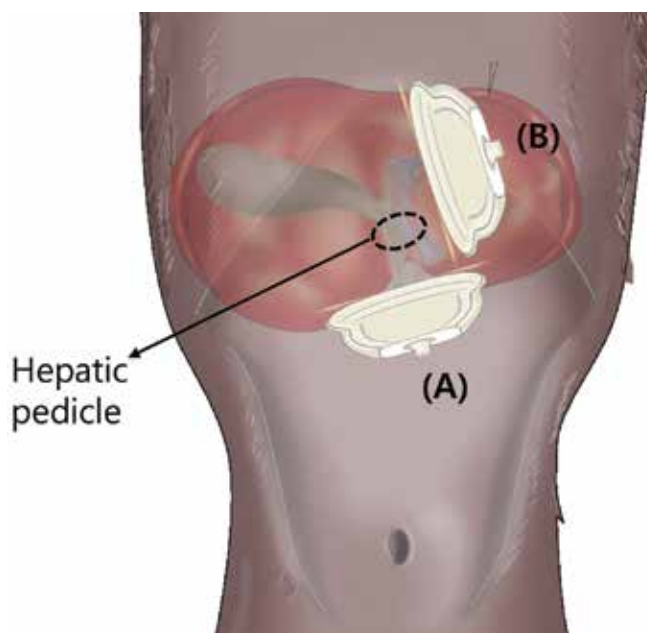


**Figure 1.** (A) To measure the diameter of vessels, the ultrasound transducer was placed perpendicular to the hepatic pedicle, and the echogenicity of the liver parenchyma was compared with that of kidney. (B) To measure the velocity within vessels, the ultrasound transducer was placed parallel with the hepatic pedicle.

artery.<sup>4</sup> The mean peak systolic velocity of the PHA was 75.4 cm/s, and the resistance index was 0.54. The mean velocity of the MPV was 19.3 cm/s.

**Differences of ultrasonographic findings according to body weight.** The diameters of the MPV and suprahepatic inferior vena cava were larger in macaques weighing more than 4.5 kg (*P* = 0.03 and 0.02, respectively). However, the diameters of the other vessels and the common bile duct did not differ significantly by body weight (Table 1). There were no significant differences in any of the other Doppler ultrasonographic findings, including PHA peak systolic velocity, PHA end-diastolic velocity, PHA resistance index, and MPV velocity (*P* = 0.07, 0.13, 0.81, and 0.24, respectively).

## Discussion

The present study addressed the ultrasonographic findings of the normal liver in cynomolgus macaques. Several important findings were described in this study: (1) the normal diameters of various vessels and the bile duct; (2) the normal flow velocities in various vessels; (3) the normal waveforms of various vessels; and (4) the normal resistance index of the PHA. In addition, Doppler ultrasonographic findings, including PHA peak systolic velocity, PHA end-diastolic velocity, PHA resistance index, and MPV velocity were independent from body weight in cynomolgus macaques. Therefore, these values can be applied to all cynomolgus monkeys, regardless of their body weight. These important findings can serve as parameters for detecting complications of liver transplantation during the early postoperative period, such as hepatic artery stenosis, portal vein stenosis, and hepatic venous outflow obstruction.<sup>3-4</sup> Furthermore, because knowing the normal ranges of each parameter is necessary for making diagnoses, this study was conducted to determine reference ranges for further research. To our knowledge, the current study represents the first ultrasonographic study of the normal liver of cynomolgus macaques. Further research aimed at determining appropriate cut-off values likely would aid the prompt diagnosis of liver transplant complications.

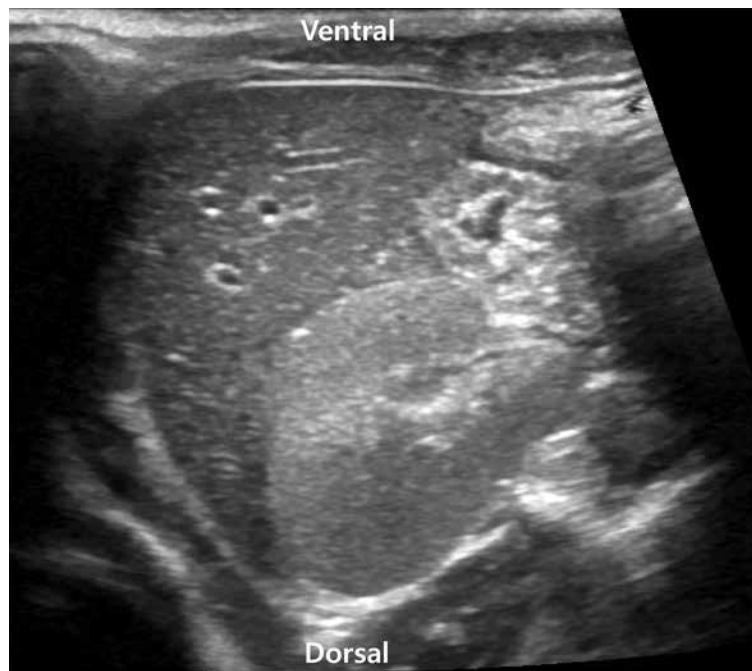


**Figure 2.** On grayscale measurement, the liver parenchyma is more hypoechoic than the kidney parenchyma.

**Table 1.** 2D ultrasonographic findings (mm; mean [range]) in healthy male cynomolgus macaques overall and according to body weight

	Overall	4.5 kg or greater ( <i>n</i> = 11)	Less than 4.5 kg ( <i>n</i> = 14)	<i>P</i>
Proper hepatic artery	1.4 (1.0–1.9)	1.5 (1.1–1.7)	1.4 (1.0–1.9)	0.44
Main portal vein	4.4 (2.4–6.0)	4.6 (3.7–6.0)	4.1 (2.4–5.3)	0.03
Right posterior portal vein	2.2 (1.2–3.3)	2.4 (1.7–3.3)	2.1 (1.2–2.8)	0.08
Right anterior portal vein	2.0 (1.3–3.0)	2.0 (1.3–2.5)	2.0 (1.5–3.0)	0.97
Left portal vein	2.1 (1.4–3.5)	2.2 (1.4–3.5)	2.0 (1.6–2.7)	0.50
Left portal vein medial branch	2.5 (1.3–3.6)	2.5 (1.3–3.5)	2.4 (1.4–3.6)	0.58
Right hepatic vein	2.3 (1.2–3.4)	2.3 (1.2–3.2)	2.2 (1.5–3.4)	0.69
Middle hepatic vein	2.4 (1.5–3.5)	2.5 (1.5–3.5)	2.2 (1.7–2.6)	0.22
Left hepatic vein	2.3 (1.4–3.1)	2.5 (1.9–3.1)	2.2 (1.4–3.1)	0.12
Suprahepatic inferior vena cava	10.6 (7.4–15.3)	11.8 (9.3–15.3)	9.7 (7.4–11.9)	0.02
Infrahepatic inferior vena cava	7.4 (5.3–10.7)	7.8 (5.3–10.7)	7.0 (5.6–10.0)	0.15
Common bile duct	1.5 (1.0–2.4)	1.6 (1.0–2.4)	1.5 (1.1–1.9)	0.50

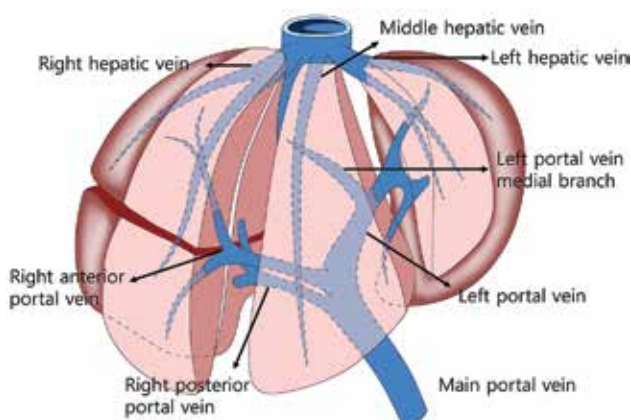


**Figure 3.** Vascular structures of the liver measured during ultrasonographic examination.

Subjects should be fasted for at least 12 h prior to ultrasonographic liver examination, because a distended stomach might cover the hepatic pedicle and impair ultrasonographic

visualization of major structures, including the MPV, PHA, and common bile duct. When the stomach is distended despite a 12-h fast, stomach contents can be removed by using a gastric tube.

We performed ultrasonographic examinations on macaques that were sedated by using ketamine (7 mg/kg) rather than anesthetized by using isoflurane. During the postoperative period after liver transplantation, frequent examinations are necessary to detect vascular and duct complications. However, general anesthesia cannot be used in every examination, because isoflurane can alter systemic hemodynamics<sup>8</sup> and thus influence the findings from ultrasonography as well as regarding the general condition of cynomolgus monkeys.<sup>4</sup>

In conclusion, the identification of normal reference values is necessary for accurately assessing the condition of the liver in cynomolgus macaques. Studying the normal conformation and structure of the liver in this species can provide useful data for correctly interpreting ultrasonographic images. An improved understanding of these images will contribute to the postoperative management of liver transplantation and the evaluation of other liver diseases. We recommend that ultrasonography of cynomolgus macaques should be performed in ketamine-sedated

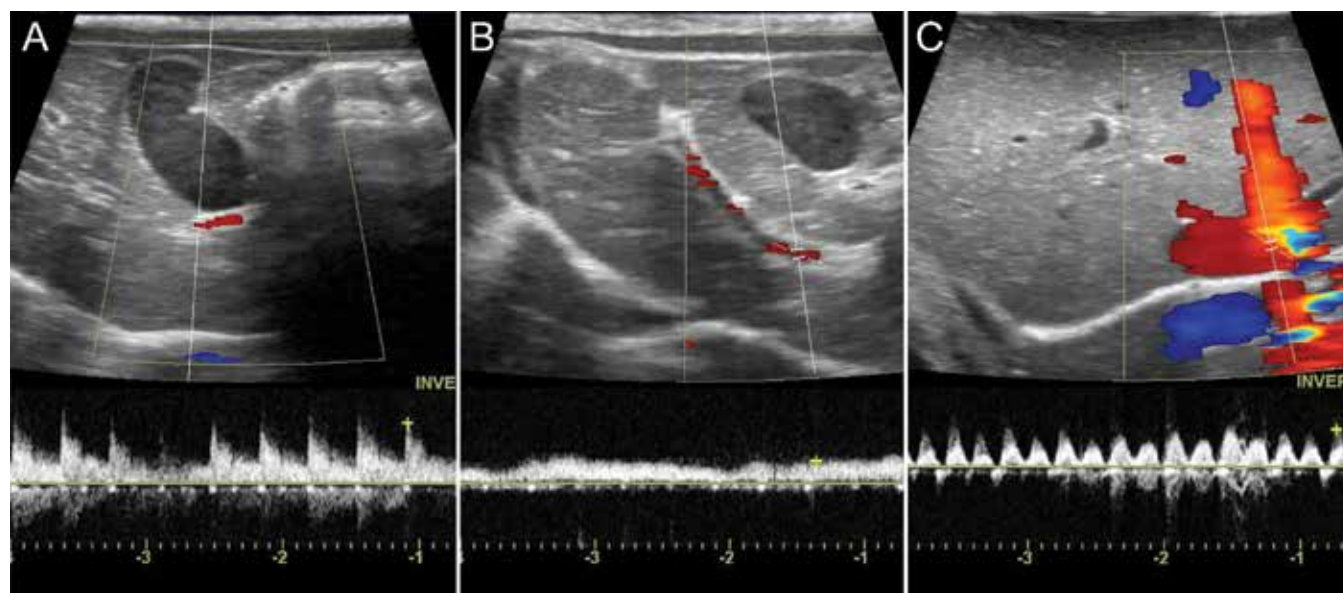


**Figure 4.** Doppler ultrasonography enables measurement of the hemodynamics of the (A) hepatic artery, (B) portal vein, and (C) hepatic vein. The hepatic artery shows a pulsatile waveform, and the portal vein yields a monophasic wave form. The hepatic vein produces a triphasic waveform.

animals that have undergone a 12-h fast, to obtain the most accurate measurements.

### Acknowledgments

This research was supported by a grant from the Korea Health Technology R&D Project through the Korea Health Industry Development Institute (KHIDI), which is funded by the Ministry of Health and Welfare, Republic of Korea (grant number HI15C2859).

### References

1. Animal Welfare Act as Amended. 2008. 7 USC §2131–2156.
2. Caiado AH, Blasbalg R, Marcelino AS, da Cunha Pinho M, Chammas MC, da Costa Leite C, Cerri GG, de Oliveira AC, Bacchella T, Machado MC. 2007. Complications of liver transplantation: multimodality imaging approach. *Radiographics* 27:1401–1417.
3. Crossin JD, Muradali D, Wilson SR. 2003. US of liver transplants: normal and abnormal. *Radiographics* 23:1093–1114.
4. Gaschen L, Menninger K, Schuurman HJ. 2000. Ultrasonography of the normal kidney in the cynomolgus monkey (*Macaca fascicularis*): morphologic and Doppler findings. *J Med Primatol* 29:76–84.
5. Institute for Laboratory Animal Research. 2011. Guide for the care and use of laboratory animals, 8th ed. Washington (DC): National Academies Press.
6. Kawai T, Leventhal J, Madsen JC, Strober S, Turka LA, Wood KJ. 2014. Tolerance: one transplant for life. *Transplantation* 98:117–121.
7. Levitsky J. 2011. Operational tolerance: past lessons and future prospects. *Liver Transpl* 17:222–232.
8. Mitchell SK, Toal RL, Daniel GB, Rohrbach BW. 1998. Evaluation of renal hemodynamics in awake and isoflurane-anesthetized cats with pulsed-wave Doppler and quantitative renal scintigraphy. *Vet Radiol Ultrasound* 39:451–458.
9. Nomura M, Yamashita K, Murakami M, Takehara M, Echizenya H, Sunahara M, Kitagawa N, Fujita M, Furukawa H, Uede T, Todo S. 2002. Induction of donor-specific tolerance by adenovirus-mediated CD40lg gene therapy in rat liver transplantation. *Transplantation* 73:1403–1410.
10. Oura T, Yamashita K, Suzuki T, Fukumori D, Watanabe M, Hirokata G, Wakayama K, Taniguchi M, Shimamura T, Miura T, Okimura K, Maeta K, Haga H, Kubota K, Shimizu A, Sakai F, Furukawa H, Todo S. 2012. Long-term hepatic allograft acceptance based on CD40 blockade by ASKP1240 in nonhuman primates. *Am J Transplant* 12:1740–1754.
11. Shah JA, Navarro-Alvarez N, DeFazio M, Rosales IA, Elias N, Yeh H, Colvin RB, Cosimi AB, Markmann JF, Hertl M, Sachs DH, Vagefi PA. 2016. A bridge to somewhere: 25-d survival after pig-to-baboon liver xenotransplantation. *Ann Surg* 263:1069–1071.
12. Vons C, Beaudoin S, Helmy N, Dagher I, Weber A, Franco D. 2009. First description of the surgical anatomy of the cynomolgus monkey liver. *Am J Primatol* 71:400–408.
13. Yamada Y, Boskovic S, Aoyama A, Murakami T, Putheti P, Smith RN, Ochiai T, Nadazdin O, Koyama I, Boenisch O, Najafian N, Bhasin MK, Colvin RB, Madsen JC, Strom TB, Sachs DH, Benichou G, Cosimi AB, Kawai T. 2011. Overcoming memory T-cell responses for induction of delayed tolerance in nonhuman primates. *Am J Transplant* 12:330–340.